

ENCIT-2018-0537

## SIMULATION OF THE AUTOTHERMAL REFORMING OF METHANE IN A FIXED BED MEMBRANE REACTOR FOR H<sub>2</sub> PRODUCTION

**Juliana Damasceno da Cruz Gouveia de Carvalho\*****Emerson Barbosa dos Anjos****Antônio Mendes da Silva Filho****Jornandes Dias Silva**Laboratory of Energetic and Environmental Technology, Polytechnic University of Pernambuco  
Benfica street, 455, 50720-001, Recife, Brazil

juliana.dcg@hotmail.com

emersonanjos@poli.br

antoniom@poli.br

jornandesdias@poli.br

**Abstract.** *Hydrogen is the most abundant chemical substance in the universe. Despite this fact, hydrogen is an energy vector and need to be produced as electricity. Among the existing methods for producing hydrogen, steam reforming is one of the most widely used. However, this technique has thermal efficiency limit since heating of large quantities of steam is required. Auto-thermal reforming of methane is an alternative to cope with this issue. In this sense, this paper aims at presenting the study, development e simulation of a mathematical model capturing the process of the auto-thermal reforming of methane in a fixed bed membrane reactor with nickel catalyst. The model is described by a set of mass and energy balances partial differential equations (EDP's), which are transformed into ordinary differential equations (EDO'S) using Coupled Integral Equations Approach (CIEA). This allows obtaining the temperatures profile data as well as evaluate CH<sub>4</sub> conversion and H<sub>2</sub> production. The results achieved suggests that the membrane performance and the steam reforming process efficiency are affected by the temperature, O<sub>2</sub>/CH<sub>4</sub> ration, H<sub>2</sub>O/CH<sub>4</sub>ratio, and pressure gradient (between reaction and permeation zones). The reactor was simulated at temperature of 837 K and pressures of 950 kPa in the reaction zone and 150 kPa in the permeation zone. The use of a fixed bed configuration makes possible to obtain an energetically self-sufficient process, capable of separating the main product with no further supporting process or even expensive units, providing a cost-effective approach to produce hydrogen.*

**Keywords:** *auto-thermal reactor, membrane, hydrogen production, process integration*

### 1. INTRODUCTION

The U.S. Energy Information Administration's (EIA, 2018) projects that world energy consumption will grow by 28% between 2015 and 2040. According to the International Energy Agency (IEA, 2018), over 70% of global energy demand growth has been met by oil, natural gas and coal. Improvements in energy efficiency along with advances within the development of renewable energy production technologies are needed. Providing the whole society with a growing energy demand is of paramount importance. Despite the still widespread burning of fossil fuels to meet energy consumption, research efforts have been made to meet the energy demand. Studies and advances in developing new technologies have focused on renewable energy production (Molina, 2017; Hernández, 2017; de Carvalho, 2017) in order to offer an alternative energy source. Fossil fuels plants have produced heat and power providing cities worldwide with steam that drives turbines and electricity to the whole society for decades. A large amount of energy comes from burning fossil fuel hydrocarbons. As a result, hydrocarbons such as carbon dioxide (CO<sub>2</sub>) and water steam (H<sub>2</sub>O) are released into the atmosphere. Global warming is largely attributed to an increase in the atmospheric level of greenhouse gases. CO<sub>2</sub> is considered as the greenhouse gas mostly influencing the climate change. Several concerns have been raised with respect to the impact in increasing carbon dioxide (CO<sub>2</sub>) concentrations in Earth's atmosphere. To mitigate the Greenhouse effect, chemical and energy industries have put effort on developing technologies to the energy production from carbon dioxide. Producing hydrogen is considered as a suitable solution to cope with the growing energy demand because it is a clean energy vector and it can be found in almost 75% of the universe. Earlier industrial interest on hydrogen was mainly triggered by the ammonia synthesis during the world wars, and then rigid policies for the diesel performance and quality, the use of hydrogen to remove sulfur from diesel are examples of its application (SOUZA, 2009).

Several processes can be used to produce hydrogen by using different renewable resources such as biomass, water and fossil fuels. In the context of hydrogen production methods from fossil fuels, steam reform (Levalley, 2014), partial oxidation (Holladay, 2009) and auto-thermal reforming (Halabi, 2008) are highlighted. This paper is focused on the later one. The steam reforming process on light hydrocarbon has been applied to produce hydrogen and synthesis gas (or syngas) in industrial-scale production. Among different types of hydrocarbon being used within the steam reforming process, the methane is the most important because it is the most plentiful high energy density chemical compound on Earth, besides the large gas supply chain. Steam reforming of methane (Ebrahimi, 2017; Settar, 2017) is the most used method for hydrogen production and syngas production. Regardless of being widely used, steam reforming is still not a thermal efficient method, since a large amount of heat is required.

Furthermore, the use of membrane reactor have been studied taking into account the concept of process intensification, in which membranes make possible both produce and separate the hydrogen within the same device, as well as operate at lower temperatures and pressure (Cruz, 2017; Gallucci, 2008; Rodríguez, 2012). The most common Palladium membranes are used within membrane reactors due to its high selectivity to hydrogen. The amount of heat needed to produce hydrogen by steam reforming of methane could represent up to 33% of the process cost due to the endothermic characteristics of the reforming reactions (de Carvalho, 2017). Using methane within the reaction reforming and combustion fuel has provided promising results in industrial applications (Rodríguez, 2012; Spallina, 2015).

In addition, catalytic steam reforming of methane (CSRSM) is the most important process to produce hydrogen. Many efforts of research have been put on using fixed-bed membrane reactors (FBMR) that allows for more efficient process, providing a better support to explore energy consumption savings (Silva, 2016; Cruz, 2017; Levalley, 2014; Galluci, 2008; Marcoberardino, 2015; Caravella, 2008; Hara, 2008; Kiriakides, 2014; Gallucci, 2013; Gil, 2015).

Advances within the steam reforming of methane have taken place on finding out the reactor design suitable to cope with the mass transfer limitations as well as the efficient thermal supply (to reactor) aiming at optimizing the process. Within this context, this paper presents a 2D-dimensional pseudo heterogeneous model to simulate and analyze the operation of a double membrane fixed bed reactor to produce hydrogen using auto-thermal steam reforming. The model is represented by a set of differential partial equations (DPE's) describing the mass and energy balance. Then, these DPE's are converted into differential ordinary equations (DOE's) by the coupled integral equation method (CIEA), and finally, these equations are solved by finite differences implemented in FORTRAN 95. Results obtained are discussed and the dynamical behavior of process is analyzed in terms of temperature profiles, components concentration, methane conversion and hydrogen production.

## 2. MATHEMATICAL MODELLING

Hydrogen is an energy vector and, henceforth, it has to be produced despite it is abundant in the universe. Several renewable resources as, e.g., biomass, water and fossil fuels, can be used to produce hydrogen. Hydrogen production methods from fossil fuels are steam reform (Levalley, 2014), partial oxidation (Holladay, 2009) and auto-thermal reforming (Halabi, 2008). The steam reforming process has been using methane to produce hydrogen and synthesis gas (or syngas) in industrial-scale production. Methane is the most plentiful high energy density chemical compound on Earth. Furthermore, there is a large gas supply chain for this hydrocarbon. Regardless of Steam reforming of methane being widely used, it is still not a thermal efficient method because a large amount of heat is required.

The focus of this paper lies on the auto-thermal methane reforming to produce hydrogen. An oxidation reaction is added into the process to supply energy for the reforming reactions, since they are endothermic. The catalytic steam reforming of methane (CSRSM) reactions (1-3), (Xu, 1989), and a fourth reaction, i.e., a water gas shift reaction (4) to enhance the production of hydrogen, are:



A fixed-bed membrane reactor with continuous flow was studied and its schematic configuration is shown in Figure 1. It consists of three concentric tubes dividing itself into the reaction zone, permeation zone and inlet oxygen zone. The oxygen is introduced into the oxygen zone, permeating through a perovskite membrane into the reaction zone where all the reactions take place. The hydrogen permeates a palladium membrane and, then, leaves the reactor through the permeation zone.

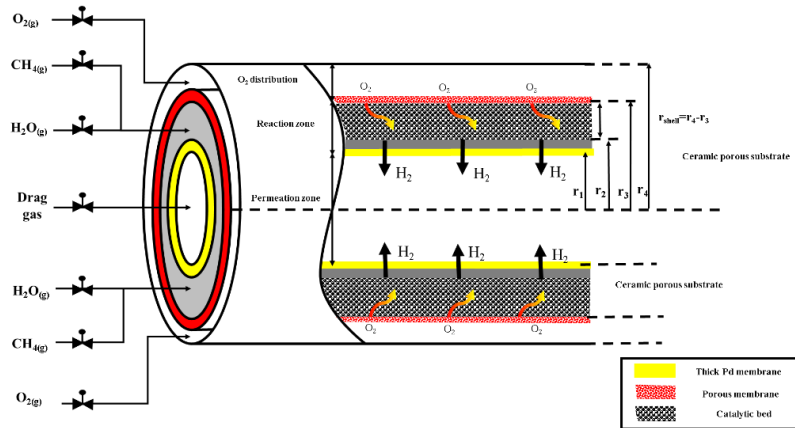


Figure 1. Schematic configuration of the FBMR

## 2.1 Mathematical issues

The models with co-current configuration can be considered as an initial value problem, so it is possible to estimate the molar concentration of  $i$  chemical components in the reactor as well as the temperature profiles in the axial and radial directions. The model of the reactor is described in terms of their energy and mass balances for the solid and gaseous phases for the  $i$  components ( $i=H_2, O_2, CO, CO_2, CH_4, H_2O$ ). For the purpose of this work, the mass and the heat transfer resistances at the gas-solid interface are also considered.

The mathematical approach used in this work had an analytical step to facilitate the equations resolutions. The CIEA method is used to transform the PDEs into ODEs. This aims at reducing the number of independent variables without the total loss of information of the variable being removed from the equation. The purpose of using this technique is to simplify presentation as well as to obtain more precise results and require less cpu time (Cardoso, 2014). After the analytical step, the equation is solved by using finite differences in our FORTRAN 95 code.

The mass and energy balances used are reported elsewhere (de Carvalho, 2017). While these balances are hydrodynamic models that describe the physical and chemical phenomena that happens in the membrane reactor, the kinetic models explain the chemical phenomena that happens during the reactions. In this context, the mathematical models can be used to evaluate some process in chemical reactors of high complexity and non-ideality conditions (Cruz and Siva 2017; Silva and Abreu, 2016).

## 2.2 Kinetic Modeling

The catalytic steam methane reforming reactions, i.e. (1)-(4), are used to develop the kinetic model (Xu and Froment, 1989; De Smet et al, 2001; Trimm and Lam, 1980). A nickel catalyst is used in this simulation due to its low cost and high activity (Hüppmeier, 2008). It is worth observing that nickel can easily deactivate by oxidation processes sintering, coking and sulfur poisoning. A possible solution is to mix nickel with other supporting substances to help minimizing these problems as, e.g. ceramic supports or  $\gamma$ -alumina, since the nickel catalysts dispersion is strongly affected by the surface area and pore size of the carrier substance (Gil et al, 2015). Catalysts based on platinum, palladium or ruthenium are generally used on ceramic (Murmura, 2016).

## 2.3 General equations for the reaction zone

The solid-gas flow conditions and complex geometries, gas transport in porous media is described by complicated mathematical models that must be simplified before resolution. For this, it was necessary to develop a mathematical model of two-dimensional steady state for the reactor (FBMR) being used. The proposed model included heat and diffusion transference phenomena in the axial and radial directions of the reactor through convection and dispersion. The gas-particle and gas-wall heat exchange are also considered. To do so, the analysis of key variables of the proposed mathematical model considers the following assumptions:

- The axial and radial chemical components flows are considered;
- The system operates on non-isothermal and steady-state conditions;
- The reaction mixture density is constant;
- The model is pseudo-heterogeneous;
- The deposition of carbon on the catalytic surface is
- The temperature of the reactor wall is considered constant;
- External mass transfer was considered within the control volume of the reactor;
- Chemical reactions occur on the surface of the catalyst;
- The gases had high surface velocity;

neglected (i.e., the deactivation of the catalyst is not expected to occur. The steam / methane ratio being used is greater than one to avoid the occurrence of this phenomenon);

- The gases have an ideal behavior;
- The bed has constant porosity in the radial and axial direction;
- The components considered in the model are CH<sub>4</sub>, H<sub>2</sub>O, CO, H<sub>2</sub>, CO<sub>2</sub> and O<sub>2</sub>;

- The Reynolds number (NRe) is estimated between 18.7 and 46.4;
- The energetic coupling between the solid and gaseous phases was carried out through the convective heat (h<sub>gs</sub>) term with their respective energy balances;
- All the considered reactions are promoted by the same catalyst;
- The particles are uniform in size;

Based on the above assumptions, the mass and energy balances of the process was analyzed and their respective governing equations are presented next.

### 2.3.1 Energy Balance in gas phase

The energy balance in the gas phase for the proposed membrane reactor is given by Equation (1):

$$\rho_{g,shell} C_{p,g,shell} \left( V_{sg,r,shell} \frac{\partial T_{g,shell}}{\partial r_{shell}} + V_{sg,z,shell} \frac{\partial T_{g,shell}}{\partial z} \right) = 2 \lambda_{g,r,shell} \frac{\partial^2 T_{g,shell}}{\partial r_{shell}^2} + \lambda_{g,z,shell} \frac{\partial^2 T_{g,shell}}{\partial z^2} - h_{gs,shell} \frac{(1-\varepsilon)}{\varepsilon} \frac{3}{R_p} (T_{g,shell} - T_{s,shell}); 0 \leq z \leq L_z, 0 \leq r_{shell} \leq R_{shell}, r_{shell} = r_3 - r_2 \quad (1)$$

Considering the Eq. (1), the first term is the convective heat flux in the radial (r) and axial (z) directions; The second term is the radial dispersion of heat (z); The third term is the axial dispersion of heat (z); The fourth term is the axial dispersion of heat (z); The fifth term is the gas-solid heat transfer; and, the sixth term is the gas-wall heat transfer. All terms of the equation are in kJ/m<sup>3</sup>h.

Eq. (1) has the following boundary conditions:

- At the FBMR's inlet (z=0);

$$\lambda_{g,z,shell} \frac{\partial T_{g,shell}}{\partial z} \Big|_{z=0^+} = \rho_{g,shell} C_{p,g,shell} V_{sg,z,shell} \left( T_{g,shell} \Big|_{z=0^+} - T_{op}^{in} \right) \quad (2)$$

- At the FBMR outlet (z=L<sub>z</sub>);

$$\frac{\partial T_{g,shell}}{\partial z} \Big|_{z=L_z} = 0 \quad (3)$$

- At the FBMR center (r<sub>shell</sub> = 0);

$$\frac{\partial T_{g,shell}}{\partial r_{shell}} \Big|_{r_{shell}=0} = 0 \quad (4)$$

- At the Diameter midpoint of the tubular membrane (r<sub>shell</sub> = d<sub>mt</sub>/2);

$$\lambda_{g,r,shell} \frac{\partial T_{g,shell}}{\partial r_{shell}} \Big|_{r_{shell}=d_{mt}/2} = h_{gs} (T_{g,shell} - T_m^{fg}) + J_{H_2} C_{p,H_2} (T_{g,shell} - T_m^{fg}) \quad (5)$$

### 2.3.2 Energy Balance in the solid phase

The energy balance in the gas phase of the proposed membrane reactor is given by Eq.(6):

$$2\lambda_{s,r,shell} \frac{\partial^2 T_{s,shell}}{\partial r_{shell}^2} + \lambda_{s,z,shell} \frac{\partial^2 T_{s,shell}}{\partial z^2} = \rho_{cat.,shell} \frac{(1-\varepsilon_p)}{\varepsilon_p} \sum_{j=1}^4 (-\Delta H_{fj,shell}) \eta_j R_j$$

$$+ h_{gs,shell} \frac{(1-\varepsilon)}{\varepsilon} \frac{3}{R_p} (T_{g,shell} - T_{s,shell}), \quad 0 \leq z \leq L_z, \quad 0 \leq r_{shell} \leq R_{shell}, \quad r_{shell} = r_3 - r_2$$
(6)

The first term is the radial heat dispersion, the second term is the axial heat dispersion, the third term is the energy whose source is the reaction itself and the fourth term is the heat transfer between the liquid and gaseous phases.

Eq.(6) has the following boundary conditions:

- At the FBMR's inlet ( $z=0$ );

$$T_{s,shell} \Big|_{z=0^+} = T_{op}^{in}$$
(7)

- At the FBMR outlet ( $z=L_z$ );

$$\frac{\partial T_{s,shell}}{\partial z} \Big|_{z=L_z} = 0$$
(8)

- At the FBMR center ( $r = 0$ );

$$\frac{\partial T_{s,shell}}{\partial r_{shell}} \Big|_{r=0} = 0$$
(9)

- At the Diameter midpoint of the tubular membrane ( $r_{shell} = d_m/2$ );

$$\lambda_{s,r,shell} \frac{\partial T_{s,shell}}{\partial r_{shell}} \Big|_{r=d_m/2} = h_{\omega} (T_{s,shell} - T_m^{fg}) + J_{H_2,shell} C_{p,H_2} (T_{s,shell} - T_m^{fg})$$
(10)

### 2.3.3 Mass Balance in the gas phase

Considering the gas phase, the chemical components are evaluated individually. Henceforth, there are mass balances for the components  $i = CH_4, H_2O, CO$  e  $CO_2$ :

$$V_{sg,r,shell} \frac{\partial C_{i,shell}}{\partial r_{shell}} + V_{sg,z,shell} \frac{\partial C_{i,shell}}{\partial z} = 2D_{ax,r,i,shell} \frac{\partial^2 C_{i,shell}}{\partial r_{shell}^2} + D_{ax,z,i,shell} \frac{\partial^2 C_{i,shell}}{\partial z^2} +$$

$$k_{gs,shell} \frac{(1-\varepsilon_{ex.})}{\varepsilon_{ex.}} \frac{3}{R_p} (C_{p,i,shell}^{surf.} - C_{i,shell}); \quad 0 \leq z \leq L_z, \quad 0 \leq r_{shell} \leq R_{shell}, \quad r_{shell} = r_3 - r_2$$
(11)

Considering the Eq. (11), the first and second terms are the convective mass flow in the radial ( $r$ ) and axial ( $z$ ) direction of the component "i" in the gas phase, respectively. The third and fourth term are the convective mass flow in the radial ( $r$ ) and axial ( $z$ ) direction of the component  $i$  in the gas phase, respectively; The fifth term are the gas-solid mass transfer.

Eq.(11) has the following boundary conditions:

- At the FBMR's inlet ( $z=0$ );

$$D_{ax,z,i,shell} \frac{\partial C_{i,shell}}{\partial z} \Big|_{z=0^+} = k_{gs,shell} (C_{i,shell} \Big|_{z=0^+} - C_{i,shell}^{in})$$
(12)

- At the FBMR outlet ( $z=L_z$ );

$$\left. \frac{\partial C_{i,shell}}{\partial z} \right|_{z=L_z} = 0 \quad (13)$$

- In the FBMR center ( $r = 0$ );

$$\left. \frac{\partial C_{i,shell}}{\partial r_{shell}} \right|_{r=0} = 0 \quad (14)$$

- In the Diameter midpoint of the tubular membrane ( $r_{shell} = d_{mt}/2$ );

$$D_{ax,r,i,shell} \left. \frac{\partial C_{i,shell}}{\partial r_{shell}} \right|_{r=d_{mt}/2} = k_{gs,shell} \left( C_{i,shell} - C_{p,i,shell}^{surf.} \right) + \frac{k_{gs,shell} P_{i,surf.}}{P_{Op}} \frac{(C_{H_2,shell} - C_{H_2,\delta})}{1 - X_{H_2,\delta}} \quad (15)$$

- At the FBMR's inlet ( $z=0$ ); Since H<sub>2</sub> and O<sub>2</sub> are elements that permeate through membranes, they have different mass balance, which are given by Eq.16:

$$\begin{aligned} V_{sg,r,shell} \frac{\partial C_{i,shell}}{\partial r_{shell}} + V_{sg,z,shell} \frac{\partial C_{i,shell}}{\partial z} &= 2 D_{ax,r,i,shell} \frac{\partial^2 C_{i,shell}}{\partial r_{shell}^2} + D_{ax,z,i,shell} \frac{\partial^2 C_{i,shell}}{\partial z^2} + \\ &\frac{(1-\epsilon_{ex.})}{\epsilon_{ex.}} \frac{3}{R_p} k_{gs,shell} \left( C_{p,i,shell}^{surf.} - C_{i,shell} \right) - \frac{\pi}{L_z} J_{i,shell} \end{aligned} \quad (16)$$

$; 0 \leq z \leq L_z, 0 \leq r_{shell} \leq R_{shell}, r_{shell} = r_3 - r_2$

The first and second terms are the convective mass flow in the radial (r) and axial (z) direction of the component "i" in the gas phase, respectively. The third and fourth term are the convective mass flow in the radial (r) and axial (z) direction of the component i at the gas phase, respectively; The fifth term is the gas-solid mass transfer; The sixth term is to the removal of H<sub>2</sub> through the palladium membrane or the passage of O<sub>2</sub> by the perovskite membrane. All terms are in (kg | m<sup>3</sup>h).

Eq.16 has the following boundary conditions:

$$D_{ax,z,i,shell} \left. \frac{\partial C_{i,shell}}{\partial z} \right|_{z=0^+} = k_{gs,shell} \left( C_{i,shell} \Big|_{z=0^+} - C_{i,shell}^{in.} \right) \quad (17)$$

- At the FBMR outlet ( $z=L_z$ );

$$\left. \frac{\partial C_{i,shell}}{\partial z} \right|_{z=L_z} = 0 \quad (18)$$

- At the FBMR center ( $r = 0$ );

$$\left. \frac{\partial C_{i,shell}}{\partial r_{shell}} \right|_{r=0} = 0 \quad (19)$$

- At the Diameter midpoint of the tubular membrane ( $r_{shell} = d_{mt}/2$ );

$$D_{ax,r,i,shell} \left. \frac{\partial C_{i,shell}}{\partial r_{shell}} \right|_{r=d_{mt}/2} = k_{gs} (C_{i,shell} - C_{i,perm}) \quad (20)$$

## 2.4 General equations for the permeation zone

Hydrogen permeation through a palladium membrane can occur through different forms depending on the type of membrane. Two assumptions made have been made: the membrane is dense, and the hydrogen transport occurs through the solution-diffusion mechanism. In addition to membrane properties, the amount of hydrogen permeating through the membrane also depends on the driving force generated by the pressure differential between the two sides of the membrane.

The recovery of the hydrogen in the permeation zone can be described through the mass and energy balances shown in equations 21 and 25, respectively:

$$\frac{dY_{H_2,per.}}{dz} = \frac{2\pi R_m L_z}{\delta_m F_{CH_4}^{in}} Q_0 \exp\left(-\frac{E_{H_2}}{RT_{av.}}\right) (P_{H_2,per.}^{0.5} - P_{H_2,shell}^{0.5}) \quad (21)$$

Eq.(21) has the following boundary conditions:

- At the FBMR's inlet (outside the permeation zone,  $z=0$ );

$$Y_{H_2,per.} \Big|_{z=0^+} = 0 \quad (22)$$

- At the FBMR's outlet (outside the permeation zone,  $z=L_z$ );

$$\left. \frac{dY_{H_2,per.}}{dz} \right|_{z=L_z} = 0 \quad (23)$$

The values of hydrogen recovery make possible to obtain the concentration of hydrogen in the permeation zone according to Eq.(24):

$$C_{H_2,per.} = \frac{P_{op}^{per.} Y_{H_2,per.}}{RT_{op}^{per.}} \quad (24)$$

$$\frac{dT_{per.}}{dz} = \frac{\pi d_{shell}}{Y_{H_2,per.} F_{H_2,0} C_{P,H_2}^{per.}} \left[ \frac{Q_0}{\delta_m} \exp\left(-\frac{E_{H_2}}{RT_{av.}}\right) (P_{H_2,per.}^{0.5} - P_{H_2,shell}^{0.5}) C_{P,H_2}^{per.} \right] (T_{g,shell} - T_{per.}) + U \frac{dT_{per.}}{dz} \quad (25)$$

Eq. (25) has the following boundary conditions:

- At the FBMR's inlet (outside the permeation zone,  $z=0$ );

$$T_{per.} \Big|_{z=0^+} = T_{per.,0} \quad (26)$$

- At the FBMR's outlet (outside the permeation zone,  $z=L_z$ );

$$\left. \frac{dT_{per.}}{dz} \right|_{z=L_z} = 0 \quad (27)$$

## 2.5 Numerical solutions

A 2D-pseudoheterogeneous model has been developed based on the mass and energy balance in different zones of the reactor for the gaseous, solid and individual phases per component (mass balance). In order to solve the mathematical modeling of the energy and mass balance equations of the gaseous and solid phases together with the boundary conditions, the Coupled Integral Equations Approach (CIEA) method (Menning, 1983; Correa, 1998; Cardoso, 2014) was applied to transform the partial differential equations (PDEs) into ordinary differential equations (ODEs). It is possible to reduce the number of independent variables without the total loss of information of the variable eliminated from the equation. The transformed equations are given next.

- Temperature in gas phase in the reaction zone:

$$\frac{d^2 \tau_{g,shell}(z)}{dz^2} + \alpha_{14,g,shell} \frac{d\tau_{g,shell}(z)}{dz} = \alpha_{15,g,shell} \tau_{g,shell}(z) + \alpha_{16,g,shell} T_m^{fg} + \alpha_{17,g,shell} \tau_{s,shell}(z) \quad (28)$$

- Temperature in solid phase in the reaction zone:

$$\frac{d^2 \tau_{s,shell}(z)}{dz^2} = \alpha_{13,s,shell} + \alpha_{14,s,shell} \tau_{g,shell}(z) + \alpha_{15,s,shell} \tau_{s,shell}(z) - \alpha_{16,s,shell} T_m^{fg} \quad (29)$$

- Concentration of  $i = \text{CH}_4, \text{H}_2\text{O}, \text{CO}, \text{CO}_2$  in the reaction zone:

$$\frac{d^2 \sigma_{i,shell}(z)}{dz^2} + \beta_{21,i,shell} \frac{d\sigma_{i,shell}(z)}{dz} = +\beta_{22,i,shell} \sigma_{i,shell}(z) + \beta_{23,i,shell} C_{p,i,shell}^{surf} + \beta_{24,i,shell} Ri \quad (29)$$

- Concentration of  $i = \text{H}_2$  e  $\text{O}_2$  in the reaction zone:

$$\frac{d^2 \sigma_{i,shell}(z)}{dz^2} + \beta_{8,i,shell} \frac{d\sigma_{i,shell}(z)}{dz} = \sigma_{i,shell}(z) \beta_{9,i,shell} + C_{i,per}(r,z) \beta_{10,i,shell} + \sigma_{p,i,shell}^{surf}(z) \beta_{11,i,shell} + \beta_{12,i,shell} Ri \quad (31)$$

## 3. RESULTS AND DISCUSSION

The investigation of auto-thermal reforming process of methane was done using a FBMR to analyze the hydrogen production, the conversion of methane as well as the temperature profiles in gas and solid phases. Figure 2 shows the catalyst temperature profiles in different radial coordinate. high temperatures have been observed near to the oxygen membrane the while lower temperatures have taken place close to the membrane center. This occurs because the higher oxygen availability closer to the perovskite membrane, resulting in a more often methane combustion. The catalyst pre-heated to 670 K, and then increased its temperature due with the exceeding heat due to methane combustion.

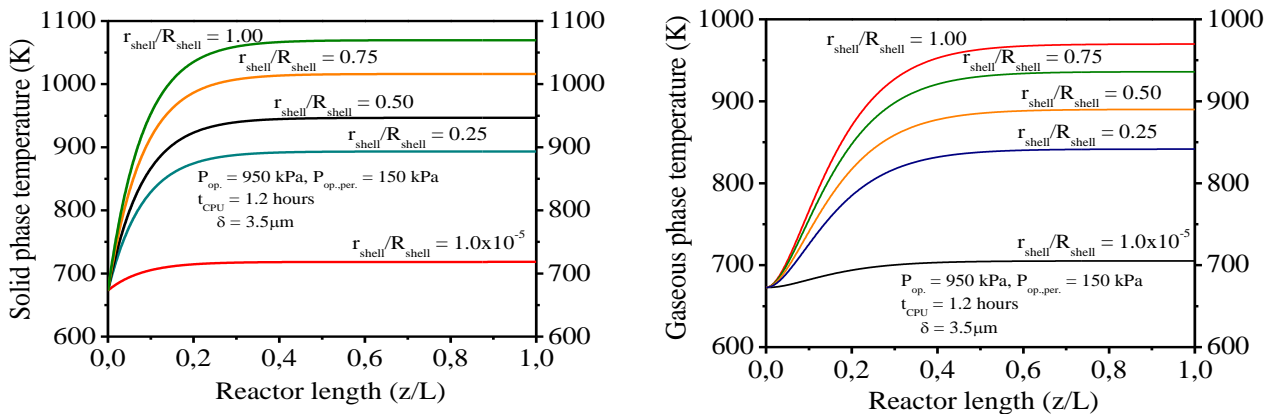


Figure 2. Profile temperatures for the solid phase (left) and for the gaseous phase (right)

Figure 3 shows the temperature profile of the gaseous phase in the reaction zone. As in Figure 2, the higher  $r_{shell}/R_{shell}$  value, the greater the proximity to the perovskite membrane. This trend is similar to the temperature profile of the solid phase: higher temperatures are observed near to the perovskite membranes. Note that the process begins at 670 K. Thus, the combustion reaction need to occur to release the necessary amount of heat for the reforming reactions and the hydrogen production. In Figure 3, no hot spots have been observed; in other words, there was not any lack or excess of energy in any area of the reaction zone. It can also be observed that in the curves with higher temperatures, the stabilization take more time when compared to the lower ones. The operation temperature is a crucial factor to ensure the process efficiency due to the endothermicity of the reforming reactions (1) and (2).

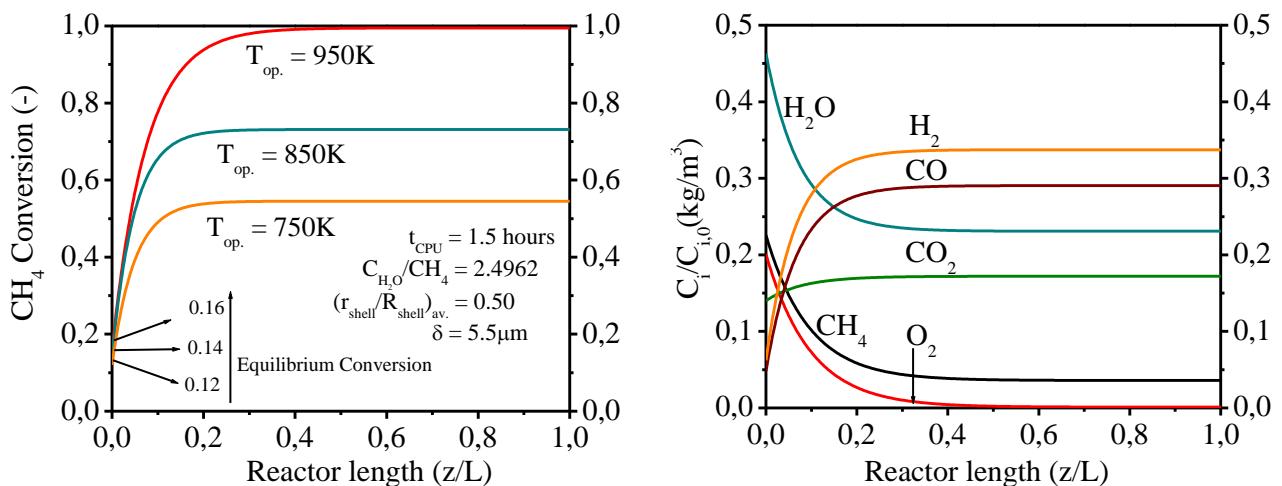


Figure 3. Methane conversion (left) and concentration profile of the components (right)

Figure 4 shows how hydrogen production evolves for different thicknesses as a function of reactor length. Note that the less the membrane thickness, the greater the hydrogen production. It is of aramount importance highlighting that as membrane thickness decreases, the hydrogen diffusion process is sped up

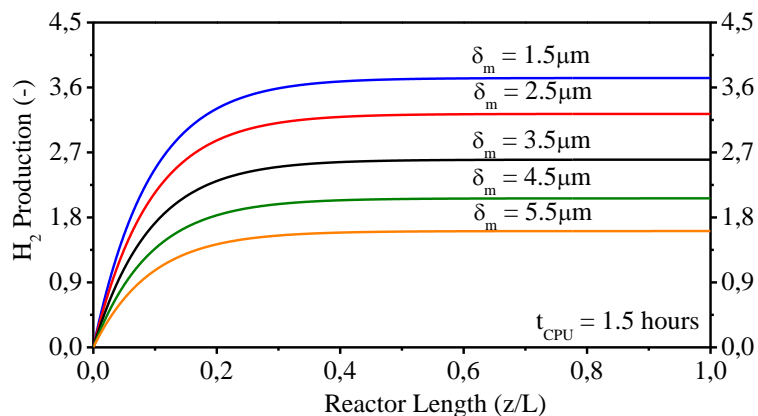


Figure 4. Hydrogen production for different membrane thicknesses

#### 4. CONCLUDING REMARKS

This work has applied a numerical methodology to analyze and appreciate the process of the autothermal methane reforming in a membrane reactor to produce hydrogen. It was possible to go through the temperatures and concentration profiles how they increase along the reactor's length and how they are distributed along the reactor ratio.

The CIEA method is a valid tool to analyze two dimensional problems, allowing the researcher to make the mass and energy balance easier to solve without the loss of information. This paper shows that is possible to investigate this technique in other kind of process in the chemistry-engineering field

This paper reports study and development of a mathematical model to analyze the hydrogen production process from the auto-thermal steam reforming of methane using an FBRM. The energy and mass balances of the process components have been specified by a set of partial differential equations, subsequently converted to ordinary differential equations by using the CIEA method. The implementation in Fortran of the numerical solution allowed to carry out simulations as well as dynamics analysis of the most important model variable behaviors, resulting in the following observations:

- i. The mathematical model of the hydrogen production auto-thermal reforming process using the FBRM allows to determine the optimal methane conversion for different O<sub>2</sub>/CH<sub>4</sub> ratio.
- ii. The study of hydrogen production was carried out by using different thickness membranes, observing that hydrogen production increases as the membrane thickness decreases.

#### 5. REFERENCES

- Caravella, A., Di Maio, F. P., Di Renzo, A., 2008. "Optimization of membrane area and catalyst distribution in a permeative-stage membrane reactor for methane steam reforming". *Journal of Membrane Science*, v. 321, p. 209-221.
- Cardoso, S. de A., Macêdo, E. N., Quaresma, J. N.N., 2014. "Improved lumped solutions for mass transfer analysis in membrane separation process of metals". *International Journal of Heat and Mass Transfer*, v. 68, p.599-611;
- Correa, E. J., Cotta, R. M., 1998. "Enhanced lumped-differential formulations of diffusion problems". *Applied Mathematical Modelling*, v. 22, p. 137-152.
- Cruz, B. M., Silva J. D., 2017. "A two-dimensional mathematical model for the catalytic steam reforming of methane in both conventional fixed-bed and fixed-bed membrane reactors for the production of hydrogen". *International Journal of Hydrogen*, v. 42, 23670 – 23690.
- De Carvalho, J. D. da C. G., 2017. "Numerical analysis of the autothermal reforming of methane to produce hydrogen in a fixed bed double membrane reactor". MSc dissertation, Polytechnic University of Pernambuco, Brazil.
- Ebrahimi, H., Rahmani, M., 2017. "Hydrogen production in membrane microreactor using chemical looping combustion: a dynamic simulation study". *Int. J. Hydrogen Energy*, v. 42, p.265-278.
- EIA 2018. "U.S. Energy Information Administration's ". 5 May, 2018 < <https://www.eia.gov/outlooks/ieo> >.
- Gallucci, F., Basile, A., 2008. "Pd-Ag membrane reactor for steam reforming reactions: a comparison between different fuels". *International Journal of Hydrogen Energy*, v. 33, p.1671-1687.
- Gallucci F., Annaland, M.V.S, 2013. "Recent advances on membranes and membranes reactors for hydrogen production". *Chemical Engineering Science*, v. 92, p. 40-66.
- Gil, A. G., Wu, Z., Chadwick, D. Li, K., 2015. "Ni/SBA-15 catalysts for combined steam reforming and water gas shift – prepared for use in catalytic membrane reactors". *Applied Catalysis A: General*, v. 506, p.188-196.
- Halabi, M. H., Croon, M.H.J.M, Van der Schaaf, J., Cobden, P.D., Schouten, J.C., 2008. "Modeling and analysis of autothermal reforming of methane to hydrogen in a fixed bed reformer". *Chemical Engineering Journal* 137, p. 568-578, 2008.

- Hara, S. et al. Reaction rate profiles in long palladium membrane reactors for methane steam reforming. *Desalination* 233, p. 359-366, 2008.
- Hernández, M.A., Lozada, F., Azcue, J. L., Torrico, J. A., Sguarezi, A. J. Battery Energy Storage System Applied to Wind Power System Based on Z-Source Inverter Connected to Grid. *IEEE Latin America Transactions*, 2016; 14: 4035-4041.
- Hinrichs, R.A., Kleibach, M. *Energia e Meio Ambiente*, Ed. Thompson.
- Holladay, et al. An overview of hydrogen production technologies. *Catalysis Today* 139, p 244-260, 2009.
- Huppmeier, J., 2008. "Interactions between reactions kinetics in ATR-reactors and transport mechanisms in functional ceramic membranes: a simulation approach". *Chemical Engineering Journal*, v.142, p. 225-238.
- IEA. "International Energy Agency" 5 May, 2018 < <https://www.iea.org/> >.
- Kiriakides, A., et al. Enhancement of pure hydrogen production through the use of a membrane reactor. *International Journal of Hydrogen Energy* 39, p. 4749-4760, 2014.
- Levalley, T. L., Richard, A. R., Fan, M. The progress in water gas shift and steam reforming hydrogen production technologies – a review. *International Journal of Hydrogen Energy* 39, p.16983-17000, 2014.
- Marcobertardino, G. et al. Fixed bed membrane reactor for hydrogen production from steam methane reforming: experimental and modeling approach. *International Journal of Hydrogen Energy* 40, 2015, p 7559-7567;
- Menning, J., Auerbach, T., Halg W. Two-point hermite approximations for the solution of linear initial value and boundary value problems. *Computer methods in applied mechanics and engineering* 39, p. 199-224, 1983.
- Molina, D.L., Vidal, J. R., Gonzáles, F. Mathematical Modeling Based on Exergy Analysis for a Bagasse Boiler. *IEEE Latin America Transactions*, 2017; 15: 65- 74.
- Rodríguez, M. I., Perdenera, M. N., Borio. D. O., 2012. "Two-dimensional modeling of a membrane reactor for ATR of methane". *Catalysis Today*, Vol. 193, 137-144.
- Settar, A., Nebbali, R., Madani, B., Abboudi, S. Numerical study on the effects of the macropatterned active surfaces on the wall-coated steam methane reformer performances. *Int. J. Hydrogen Energy*, 2017; 42: 1490-1498.
- Silva, J. D., Abreu, C. A. M. Modelling and simulation in conventional fixed-bed and fixed-bed membrane reactors for the steam reforming methane. *International Journal of Hydrogen Energy* 41, p. 11660-11654, 2016.
- Spallina, V., Melchiori, T., Gallucci, F., Annaland, M. S., 2015. "Autothermal reforming using mixed ion-electronic conducting ceramic membranes for a small-scale production plant". *Molecules*, Vol. 20, p. 4998 – 5023.
- Souza, M. M. V. M. *Hydrogen technology*, Synergia, 2009
- Xu, J., Froment, G.F., 1989. "Methane steam reforming, methanation and water-gasshift: I. Intrinsic kinetics". *Aiche Journal*, v. 35: p. 88-96.

## 6. RESPONSIBILITY NOTICE

The authors are the only responsible for the printed material included in this paper.